ChemComm

Cite this: *Chem. Commun.*, 2012, **48**, 10416–10418

www.rsc.org/chemcomm

**COMMUNICATION**

# Reengineered epipodophyllotoxin†

**Igor V. Magedov,*[a] Nikolai M. Evdokimov,[a] Menuka Karki,[b] Amanda S. Peretti,[c] Dustin T. Lima,[a] Liliya V. Frolova,[a] Mary R. Reisenauer,[c] Anntherese E. Romero,[c] Paul Tongwa,[d] Alexandr Fonari,[d] Jeff Altig,[a] Snezna Rogelj,[c] Mikhail Yu. Antipin,[d] Charles B. Shuster[b] and Alexander Kornienko*[ae]**

***Received 14th July 2012, Accepted 29th August 2012***
**DOI: 10.1039/c2cc35044k**



**A variant structural skeleton of epipodophyllotoxin was synthesized and found to rival the natural cyclolignan in antiproliferative and microtubule destabilizing properties. This discovery leads to a new structural class of tubulin targeting agents.**

Cyclolignan podophyllotoxin (**1**, Fig. 1), isolated from American mayapple (*Podophyllum peltatum*), was extensively investigated as an antitumor agent, but the clinical results were disappointing due to severe gastrointestinal side effects.[1] Its C-4 epimer epipodophyllotoxin (**2**), also found in the above-mentioned plant,[2] is generally 5–10 times less potent as an antiproliferative agent against cancer cells and as an inhibitor of *in vitro* mitotic spindle assembly.[1,3–8]

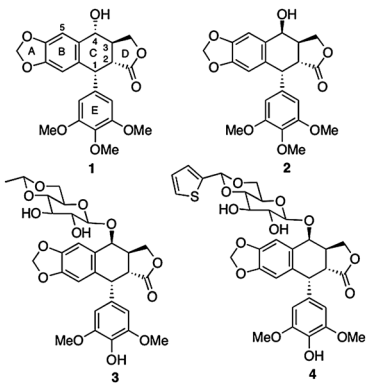

**Fig. 1** Structures of podophyllotoxin (**1**), epipodophyllotoxin (**2**), etoposide (**3**) and teniposide (**4**).

[a] *Department of Chemistry, New Mexico Institute of Mining and Technology, Socorro, New Mexico 87801, USA. E-mail: imagedov@nmt.edu*
[b] *Department of Biology, New Mexico State University, Las Cruces, New Mexico 88003, USA*
[c] *Department of Biology, New Mexico Institute of Mining and Technology, Socorro, New Mexico 87801, USA*
[d] *Department of Biology and Chemistry, New Mexico Highlands University, Las Vegas, New Mexico 87701, USA*
[e] *Department of Chemistry and Biochemistry, Texas State University – San Marcos, San Marcos, TX 78666, USA. E-mail: a_k76@txstate.edu*

† Electronic supplementary information (ESI) available: Synthetic procedures, molecular biology methods, X-ray data, details of tubulin polymerization assay and computational work. CCDC 873143–873145. For ESI and crystallographic data in CIF or other electronic format see DOI: 10.1039/c2cc35044k

However, its glycosylated derivatives etoposide (**3**) and teniposide (**4**), commonly referred to as epipodopyllotoxins, are currently used in clinics for the treatment of lung and testicular cancers, lymphoma, non-lymphocytic leukemia and glioblastoma multiforme.[3] Due to the development of drug resistance by cancer cells as well as side effects associated with the use of these agents in clinics, the search for new effective anticancer drugs with **1** and **2** as lead agents remains an intense area of research.[4–6]

Unfortunately, the complex chemical structure of podophyllotoxin prevents the generation of libraries of its analogues from simple commercially available materials. At the same time, the derivatization of podophyllotoxin as a means to obtain structure–activity relationship (SAR) information has the drawback of producing non-systematic data because it is limited by the type of chemistry that podophyllotoxin can undergo. For example, substitutions of rings AB and E by other moieties have been scarcely explored due to the synthetic challenge of removing the profuse oxygenation in these parts of the molecule (Fig. 2). Limited literature examples include ring E phenyl analogue **5** synthesized by Berkowitz and co-workers in 19 steps from commercially available materials[9] and phenazine **6** prepared by way of oxidation of the AB subunit to an *ortho*-quinone and its subsequent condensation with 1,2-phenylenediamine.[10] These reports constitute rare synthetic accomplishments illustrating the challenge of a systematic exploration of the chemical space occupied by these oxygenated moieties.[11]

Computer modeling simulations utilizing the tubulin–podophyllotoxin crystal structure[12] revealed that the

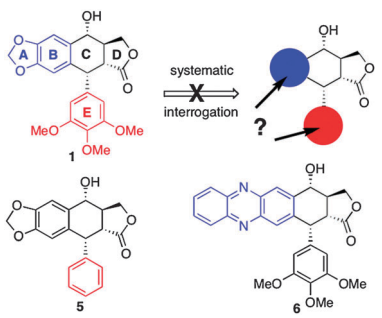


**Fig. 2** Is systematic interrogation of the chemical space occupied by rings AB and E possible?

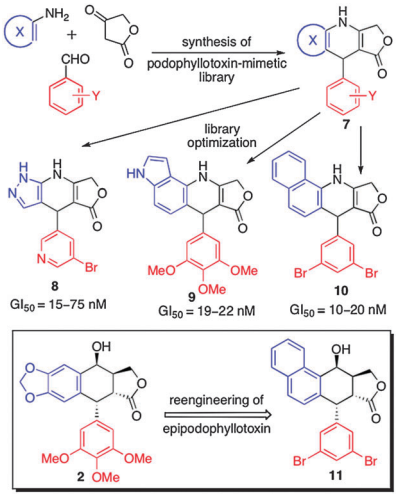


**Fig. 3** Strategy leading to reengineered epipodophyllotoxin **11**.

podophyllotoxin's pentacyclic framework can be mimicked with a dihydropyridine-based scaffold having comparable binding modes at the colchicine site.[13] Because this mimetic dihydropyridine skeleton is easily accessible by a multicomponent reaction (MCR) of commercially available aromatic/heteroaromatic amines with aldehydes and tetronic acid, we prepared a diverse library of podophyllotoxin mimetics and generated systematic anticancer SAR data.[13] In this method, the utilization of selected amine and aldehyde starting materials leads directly to the desired modifications of rings AB and E, respectively (Fig. 3). We found that compounds incorporating pyrazole (**8**), indole (**9**) and naphthalene (**10**) AB ring substitutions possessed nanomolar antiproliferative potencies. In addition, the trimethoxy substitution of ring E was not critical as 3-bromopyridine and 3,5-dibromophenyl rings were superior in many cases (*e.g.*, **8** and **10**). Although our MCR-based mimetic scaffold approach led to promising novel antitubulin agents (*i.e.*, **8**, **9** and **10**) in its own right, we were intrigued by the possibility of utilizing this method as a tool to rapidly probe drastic skeleton modifications in the natural cyclolignans. With this idea in mind, we conceived reengineered epipodophyllotoxin **11**, whose new naphthalene and 3,5-dibromophenyl rings AB and E were inspired by the MCR product **10**. In this communication, we report synthesis and anticancer evaluation of this unorthodox epipodophyllotoxin analogue.

The synthesis relied on an *exo*-selective intramolecular Diels–Alder reaction of ester **17**, prepared using standard chemistry (Scheme 1). A simple reflux of **17** in toluene gave a 1.6 : 1 mixture of *exo* and *endo* products **18** and **19**. These were easily separable and their structures were confirmed by single-crystal X-ray analyses. The desired C-4 hydroxyl was installed by the dihydroxylation of **18**, which proceeded exclusively from the β-face furnishing diol **20** as a single diastereomer (Scheme 2). The synthesis of the epipodophyllotoxin analogue **11** was then completed by a TFAA-promoted dehydration to give dihydronaphthalene **21** and its subsequent oxidation with DDQ. The structure of **11** was unambiguously established with X-ray crystallography. The synthetic work was completed by the preparation of additional analogues in the *cis*-lactone series. To this end, *endo* Diels–Alder product **19** was subjected to the same three-reaction sequence leading to *cis*-lactone **24**.

Evaluation of the synthesized analogues for antiproliferative activity was performed using HeLa and MCF-7 cancer cell lines as models for human cervical and breast adenocarcinomas, respectively (Table 1). In addition, we assessed the ability of these compounds to induce apoptosis in Jurkat cells

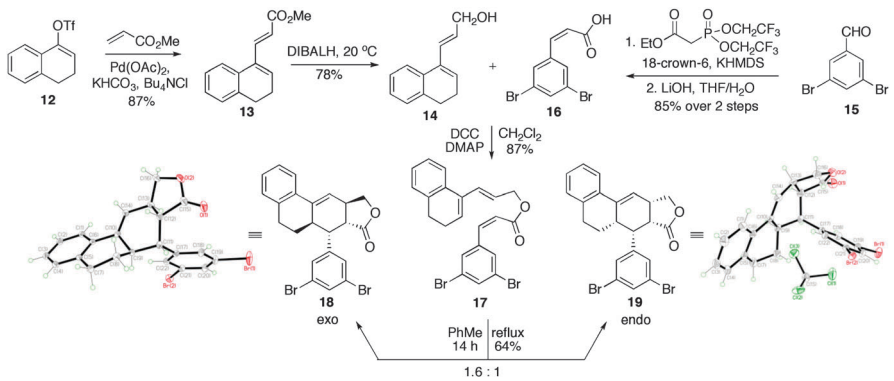


**Scheme 1** Synthesis of Diels–Alder products **18** (*exo*) and **19** (*endo*).

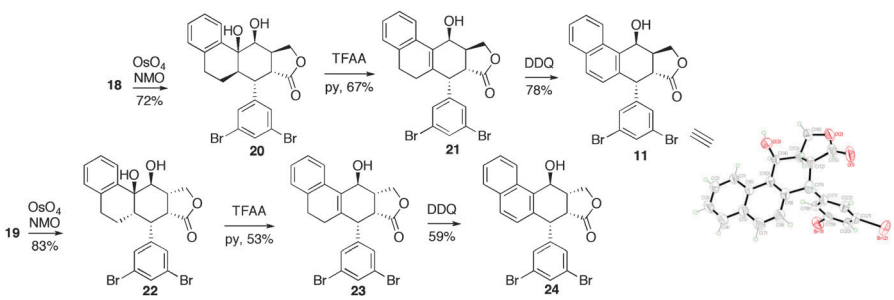


**Scheme 2** Elaboration of the Diels–Alder products **18** and **19** to reengineered epipodophyllotoxin **11** and its C-3 epimer **24**.

**Table 1** Antiproliferative and apoptosis-inducing properties of the synthesized compounds, and their binding energies at the colchicine site

| # | $GI_{50}$[a]/μM HeLa | $GI_{50}$[a]/μM MCF-7 | Apoptosis (%) Jurkat | Binding energies[c]/kJ mol$^{-1}$ |
|---|---|---|---|---|
| **1** | 0.030 ± 0.002 | 0.018 ± 0.002 | 37.5 ± 1.9 | −9.3 |
| **2** | 0.36 ± 0.09 | 0.24 ± 0.00 | 30.0 ± 1.2 | −9.2 |
| **10** | 0.016 ± 0.002 | 0.014 ± 0.001 | 27.7 ± 3.2 | −8.1 |
| **18** | 30.8 ± 7.9 | 23.7 ± 0.8 | 8.0 ± 1.3 | nd |
| **19** | 3.4 ± 0.1 | 4.4 ± 0.2 | 7.0 ± 1.0 | −7.0 |
| **20** | 42.2 ± 1.0 | 46.9 ± 0.7 | 7.5 ± 0.4 | nd |
| **21** | 0.22 ± 0.00 | 0.23 ± 0.01 | 28.5 ± 1.3 | −8.6 |
| **11** | 0.56 ± 0.01 | 0.43 ± 0.05 | 39.7 ± 0.8 | −8.4 |
| **22** | 56.9 ± 3.4 | 79.7 ± 0.1 | 7.3 ± 0.6 | nd |
| **23** | 41.4 ± 3.0 | 24.1 ± 1.4 | 7.7 ± 1.4 | nd |
| **24** | 12.9 ± 2.4 | 5.9 ± 0.1 | 7.4 ± 0.7 | nd |

[a] Concentration required to reduce the viability of cells by 50% after 48 h of treatment with indicated compounds, relative to DMSO control ± SD, determined by MTT assay. [b] % Apoptotic cells after 24 h of treatment with indicated compounds at the concentration of 300 nM relative to DMSO control ± SD, determined by flow cytometric Annexin-V/propidium iodide assay. [c] Binding energies revealed by Autodock Vina simulations, nd = no comparable binding pose.

(a model for human T-cell leukemia) and calculated their binding energies using docking simulations (Table 1). The results indicated that in accordance with the literature data **2** was about an order of magnitude less potent in its antiproliferative effects than **1**. Analogue **11**, together with its dihydronaphthalene variant **21**, exhibited submicromolar antiproliferative activity and potent apoptosis-inducing properties rivaling those of **2**, in spite of their racemic nature. In addition, these four compounds displayed good binding affinities as revealed by Autodock simulations. This can also be seen in Fig. 4 visually demonstrating that the matching enantiomer of reengineered epipodophyllotoxin **11** and its dihydronaphthalene

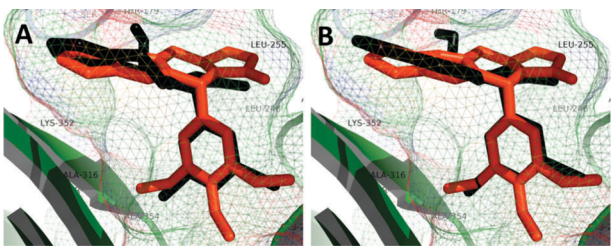


**Fig. 4** Molecular docking poses (black) of **21** (A) and **11** (B) overlaid with that of **1** (red).

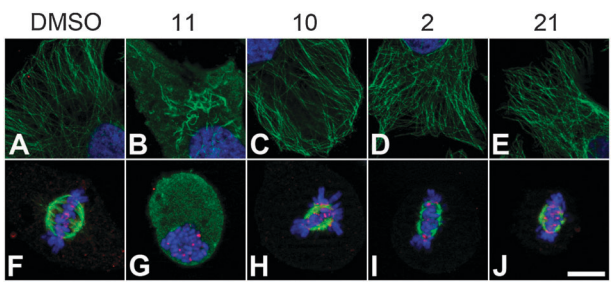


**Fig. 5** Microtubule organization in HeLa cells during interphase (A–E) and mitosis (F–J). Hela cells were treated for 3 hours with the indicated compounds at their MTT-related $GI_{50}$ concentrations (see Table 1). Following drug treatment, cells were probed for microtubules (green), centromeres (red) and DNA (blue). Bar, 10 μ.

analogue **21** bound to the colchicine site in orientations similar to that of **1**. It should be noted that *cis*-lactone derivatives are significantly less active as revealed by literature reports[4–6] as well as the results of the present investigation demonstrating decreased activity associated with *cis*-lactone analogues **22–24** and the absence of comparable binding modes in docking simulations.

Our mechanistic experiments confirm that compounds **21** and **11** retain the antitubulin mode of action of epipodophyllotoxin. Thus, **11** was found to arrest cancer cells in the G2/M phase of the cell cycle, exhibit little toxicity toward normal primary blood lymphocytes and (together with **21**) display microtubule-destabilizing activity *in vitro* using a fluorimetry-based tubulin polymerization assay[13] (see ESI† for details). In addition, to determine the extent of microtubule disruption in whole cells, HeLa cells were cultured in the presence of a carrier control (DMSO) or compounds **2**, **10**, **11** and **21** at the half maximal growth inhibitory concentration and examined for microtubule morphology (Fig. 5). In contrast to DMSO-treated cells that displayed normal interphase and mitotic microtubule organization (A and F), compounds **2**, **10**, **11** and **21** all affected spindle morphology (G–J). Reengineered epipodophyllotoxin **11** exhibited the most potent destabilizing activity, completely blocking spindle formation (G) and disrupting all but the most stable microtubules in interphase cells (B). Compounds **10**, **2** and **21** had no effect on the relatively stable interphase microtubules (C–E), but did result in shorter spindle lengths, as evidenced by 13, 7.5 and 15.2% decreases in pole-to-pole distances, respectively (H–J).

In conclusion, using our MCR-based mimetic scaffold approach we conceived and synthesized an epipodophyllotoxin analogue possessing a variant structural skeleton. Despite being racemic, this compound rivals the natural cyclolignan in its antiproliferative and apoptosis-inducing properties and induces dramatic microtubule disorganization effects in whole cells. Thus, compound **11** represents a new structural class of tubulin targeting agents.

## Notes and references

1 T. F. Imbert, *Biochimie*, 1998, **80**, 207–222.
2 J. K. Bastos, C. L. Burnadt, N. P. D. Nanayakkara, L. Bryant and J. D. McChesney, *J. Nat. Prod.*, 1996, **59**, 406–408.
3 L. Bohlin and B. Rosen, *Drug Discovery Today*, 1996, **1**, 343–351.
4 Y. J. You, *Curr. Pharm. Des.*, 2005, **11**, 1695–1717.
5 M. Gordaliza, M. A. Castro, J. M. M. Corral and A. San Feliciano, *Curr. Pharm. Des.*, 2000, **6**, 1811–1839.
6 M. Lv and H. Xu, *Mini-Rev. Med. Chem.*, 2011, **11**, 901–909.
7 M. Gordaliza, M. A. Castro, M. D. Garcia-Gravalos, P. Ruiz, J. M. M. del Corral and A. San Feliciano, *Arch. Pharm. (Weinheim, Ger.)*, 1994, 175–179.
8 C. F. Brewer, J. D. Loike, S. B. Horwitz, H. Sternlicht and W. J. Gensler, *J. Med. Chem.*, 1979, **22**, 215–221.
9 D. B. Berkowitz, J.-H. Maeng, A. H. Dantzig, R. L. Shepard and B. H. Norman, *J. Am. Chem. Soc.*, 1996, **118**, 9426–9427.
10 S. J. Cho, Y. Kashiwada, K. F. Bastow, Y. C. Cheng and K.-H. Lee, *J. Med. Chem.*, 1996, **39**, 1396–1402.
11 For related pyridazine and indole A,B-ring analogues, see (*a*) E. Bertounesque, T. Imbert and C. Monneret, *Tetrahedron*, 1996, **52**, 14235–14246; (*b*) S. D. Cline, T. L. Macdonald and N. Osheroff, *Biochemistry*, 1997, **36**, 13095–13101.
12 R. B. J. Ravelli, B. Gigant, P. A. Curmi, I. Jourdain, S. Lachkar, A. Sobel and M. Knossow, *Nature*, 2004, **428**, 198–202.
13 I. V. Magedov, L. Frolova, M. Manpadi, U. D. Bhoga, H. Tang, N. M. Evdokimov, O. George, K. H. Georgiou, S. Renner, M. Getlic, T. L. Kinnibrugh, M. A. Fernandes, S. van Slambrouck, W. F. A. Steelant, C. B. Shuster, S. Rogelj, V. L. A. van Otterlo and A. Kornienko, *J. Med. Chem.*, 2011, **54**, 4234–4246, and references cited therein.

 